Supporting Information for

Investigation of organic hydrotrioxides (ROOOH) formation from RO_2 + OH reactions and their atmospheric impact by a chemical transport model, STOCHEM-CRI

M. Anwar H. Khan[a,*], Rayne Holland[a], Asan Bacak[b,c], Thomas J. Bannan[d], Hugh Coe[d,e], Richard G. Derwent[f], Carl J. Percival[g], Dudley E. Shallcross[a,h,*]

[a]Atmospheric Chemistry Research Group, School of Chemistry, University of Bristol, Bristol, UK

[b]Ankara University Cancer Research Institute, Balkiraz Mahallesi, Mamak Caddesi No:1/8, Mamak, Ankara, Turkey

[c]Turkish Accelerator & Radiation Laboratory, Ankara University, Golbasi, Ankara, Turkey

[d]Department of Earth and Environmental Science, Centre for Atmospheric Science, University of Manchester, Manchester, UK.

[e]National Centre for Atmospheric Sciences, University of Manchester, Manchester, UK

[f]rdscientific, Newbury, UK

[g]Jet Propulsion Laboratory, California Institute of Technology, 4800 Oak Grove Dr, Pasadena, CA 91109, USA

[h]Department of Chemistry, University of the Western Cape, Robert Sobukwe Road, Bellville 7305, South Africa

*Corresponding authors: M Anwar H Khan (anwar.khan@bristol.ac.uk) and Dudley E. Shallcross (d.e.shallcross@bristol.ac.uk)

Contents of this file

Table S1-S5, Figures S1-S3

Table S1. The production of ROOOH and ROH from the reaction R11b and R11d

CRI species name of RO2	MCM species name of RO2	Contribution to ROOOH (Tg/yr)	Contribution to ROH (Tg/yr)
CH3O2	CH3O2	67.51	55.24
C2H5O2	C2H5O2	0.84	0.81
IC3H7O2	IC3H7O2	0.10	0.11
HOC2H4O2	HOC2H4O2	0.22	0.24
CH3CO3	CH3CO3	4.78	5.11
C2H5CO3	C2H5CO3	0.06	0.07
HOCH2CO3	HOCH2CO3	0.48	0.56
MACO3	MACO3	0.10	0.13
RN19O2	HEXCO2, M2PEDO2, M3PECO2	0.01	0.01
RN18O2	C65OH4O2, C6OH5O2, HO2C6O2	<0.01	<0.01
RN17O2	HEX3ONAO2, EIPKAO2, M2BKAO2	0.01	0.01
RN16O2	PEAO2, PEBO2, PECO2	0.05	0.06
RN15O2	C51OH2O2, C52OH3O2, HO2C5O2	<0.01	<0.01
RN14O2	MPRKBO2, DIEKAO2, MIPKAO2	0.03	0.03
RN13O2	NC4H9O2	0.67	0.76
RN12O2	HO1C4O2, BUT2OLO2	0.15	0.19
RN11O2	MEKAO2, MEKBO2, BUTALO2	0.41	0.49
RN10O2	NC3H7O2	0.06	0.06
RN9O2	HYPROPO2, IPROPOLO2	0.05	0.06
RN8O2	PROPALO2, CHOC2H4O2	0.66	0.75
RN13AO2	SC4H9O2	0.02	0.02
RN16AO2	C6CO3OH5O2, C69O2	<0.01	<0.01
RN15AO2	HO1C5O2	0.08	0.11
RN18AO2	HO3C6O2, HO2M2C5O2	<0.01	0.01
NRN12O2	C42NO33O2	<0.01	<0.01
NRN9O2	PR1O2NO3, PR2O2NO3	<0.01	<0.01
NRN6O2	ETHO2NO3	<0.01	<0.01
RU14O2	ISOPAO2, ISOPBO2, ISOPCO2, ISOPDO2	2.51	3.12

RU12O2	C57O2, C58O2, C59O2, HC4ACO3, HC4CCO3	1.62	2.14
RU10O2	MACRO2, MACROHO2, MACO3, HMVKAO2, HMVKBO2	1.06	1.33
NRU14O2	NISOPO2	0.05	0.06
NRU12O2	C510O2, NC4CO3	0.22	0.30
RU12AO2	MACRO2	0.03	0.04
DHPR12O2	C536O2, C537O2	0.01	0.02
RTN28O2	APINAO2, APINBO2, APINCO2	0.15	0.20
RTN26O2	PINALO2	0.26	0.37
RTN25O2	C96O2	0.68	0.93
RTN24O2	C97O2	0.68	0.94
RTN23O2	C98O2	0.74	1.03
RTN14O2	C614O2	0.60	0.80
RTN10O2	CO23C4CO3	0.38	0.50
NRTN28O2	NAPINAO2, NAPINBO2	0.04	0.05
RTX28O2	BPINAO2, BPINBO2, BPINCO2	0.22	0.30
RTX24O2	NOPINAO2, NOPINBO2, NOPINCO2, NOPIDO2	0.19	0.25
RTX22O2	C915O2, C917O2, C918O2, C89CO3	0.22	0.30
NRTX28O2	NBPINAOOH, NBPINBOOH	0.09	0.12
RA16O2	TLBIPERO2	0.04	0.05
RA13O2	BZBIPERO2	0.03	0.04
RA19AO2	OXYBIPERO2	0.02	0.02
RA19CO2	OXYLO2	<0.01	0.01

Note: Structures of the species can be obtained using species name and search facility on MCM website (https://mcm.york.ac.uk/MCM/).

Table S2. Losses of OH by different species

Species	Loss (s^{-1})	% contribution
Volatile Organic Compounds	1.56	65
Carbon monoxide	0.37	15
NOz	0.24	10
H_2	0.07	3
H_2O_2	0.05	2
RO_2	0.05	2
O_3	0.05	2
HO_2	0.02	1

Table S3. Comparison of measured and modelled OH reactivity

Location	Time	Longitude, Latitude	Observed OH reactivity (s^{-1})	Modelled OH reactivity (s^{-1})
Whiteface Mountain,USA[1]	Jul-Aug	44N,73W	5.6	5.1
Nashville, USA[2]	Jun-Jul	36N,86W	11.3	10.8
Borneo, Malaysia[3]	AprMay	4N,117E	15.3	7.8
Amazon, Brazil[4]	Nov	2S,58W	17.1	14.2
Amazon, Brazil[4]	Feb-Mar	2S,58W	9.5	15.9
Amazon, Brazil[4]	Jun	2S,58W	26.2	21.5
Amazon, Brazil[4]	Sep	2S,58W	53.7	13.2
Weybourne, UK[5]	May	52N,1E	4.9	5.8
Yufa, China[6]	Sep	39N,116E	19.7	6.5
Backgarden, China[7]	July	23N,113E	31.4	7.7
Brownsberg, Surinam[8]	Oct	4N,55W	53	11.5
Mainz, Germany[8]	Aug	49N,8E	10.4	5.3
Jülich, Germany[9]	Jul	50N,6E	8.6	5.2
Heshan, China[10]	Oct-Nov	22N,112E	30.6	4.3
Beijing, China[10]	Aug	39N,116E	20	5.5
Ersa, Corsica[11]	Jul-Aug	42N,9E	5	3.7
New York, USA[12]	Jul	40N,73W	19	5
New York, USA[13]	Jan	40N,73W	25.1	6.5
Pennsylvania, USA[14]	May-Jun	40N,77W	6.1	5.7
Mexico city, Mexico[15]	Apr	19N,99W	47.5	5
Houston, USA[16]	Aug-Sep	29N,95W	9.4	3.7
La porte, Texas[16]	Aug-Sep	29N,95W	12.24	4.5
Paris, France[17]	Jan-Feb	48N,2E	40.3	4.6
Lilli, France[18]	Oct	50N,3E	7.4	3.8
London, UK[19]	Jul-Aug	51N,0W	18.1	4.4
Michigan, USA[20]	Jul-Aug	45N,84W	7.8	6.1
Hyytiälä, Finland[21]	Aug	61N,24W	8.6	2.4
Hyytiälä, Finland[22]	Jul-Aug	61N,24W	11.5	3.1
Rocky Mountain, USA[23]	Aug	39N,105W	6.7	3.2
Haute Provence, France[24]	May-Jun	43N,5E	17.9	4.3
Alabama, USA[25]	Jun-Jul	32N,87W	19.4	12.4
California, USA[26]	Jun-Jul	39N,120W	17.3	3.4
North Pacific[27]	Apr_May	20-60N,120-180W	4	1.1
Arabian Peninsula[28]	Jul-Aug	40-60N,0-60W	7.2	1.6
Shanghai, China[29]	Aug-Sep	31N,120W	38.4	4.6

Note: [1]Ren et al. (2006a), [2]Kovacs et al. (2003), [3]Edwards et al. (2013), [4]Nölscher et al. (2016), [5]Lee et al. (2009), [6]Lu et al. (2010), [7]Lou et al. (2010), [8]Sinha et al. (2008), [9]Elshorbany et al. (2012), [10]Yang et al. (2017), [11]Zannoni et al. (2017), [12]Ren et al. (2003), [13]Ren et al. (2006b), [14]Ren et al. (2005), [15]Shirley et al. (2006), [16]Mao et al. (2010), [17]Dolgorouky et al. (2012), [18]Hansen et al. (2015), [19]Whalley et al. (2016), [20]Hansen et al. (2014), [21]Sinha et al. (2010), [22]Nölscher et al. (2012), [23]Nakashima et al. (2014), [24]Zannoni et al. (2016), [25]Kaiser et al. (2016), [26]Mao et al. (2012), [27]Mao et al. (2009), [28]Pfannerstill et al. (2019), [29]Yang et al. (2022).

Table S4 : Annual tropospheric loss fluxes of the reactions of RO_2 with NO, NO_3, HO_2, RO_2 and OH

Species	**Flux (molecules/yr)**				
	RO2+NO	**RO2+NO3**	**RO2+HO2**	**RO2+RO2**	**RO2+OH**
CH3O2	1.81×10^{37}	2.16×10^{35}	1.66×10^{37}	1.32×10^{36}	5.77×10^{36}

C2H5O2	4.30×10^{35}	3.75×10^{33}	2.41×10^{35}	4.40×10^{33}	5.88×10^{34}
RN10O2	3.33×10^{34}	1.91×10^{32}	2.61×10^{34}	5.33×10^{32}	3.56×10^{33}
IC3H7O2	4.35×10^{34}	3.84×10^{32}	3.94×10^{34}	5.69×10^{31}	5.85×10^{33}
RN13O2	3.82×10^{35}	3.48×10^{33}	2.83×10^{35}	2.21×10^{33}	3.45×10^{34}
RN16O2	2.19×10^{34}	2.10×10^{32}	1.95×10^{34}	1.28×10^{32}	2.10×10^{33}
RN19O2	8.34×10^{33}	5.62×10^{30}	3.62×10^{33}	4.13×10^{31}	3.30×10^{32}
RN13AO2	1.77×10^{34}	1.87×10^{31}	7.90×10^{33}	3.04×10^{32}	9.58×10^{32}
RN16AO2	8.98×10^{32}	9.10×10^{30}	7.83×10^{32}	2.30×10^{31}	8.39×10^{31}
RA13O2	8.50×10^{33}	8.64×10^{31}	8.99×10^{33}	1.66×10^{32}	8.58×10^{32}
RA16O2	2.06×10^{34}	1.70×10^{32}	1.19×10^{34}	8.14×10^{31}	1.09×10^{33}
RA19AO2	1.16×10^{34}	9.28×10^{31}	4.99×10^{33}	1.36×10^{32}	4.48×10^{32}
RA19CO2	4.95×10^{33}	3.98×10^{31}	2.14×10^{33}	5.81×10^{31}	1.92×10^{32}
HOCH2CH2O2	1.94×10^{35}	1.45×10^{33}	1.04×10^{35}	6.86×10^{33}	1.29×10^{34}
RN9O2	4.48×10^{34}	3.80×10^{32}	1.86×10^{34}	1.01×10^{33}	2.60×10^{33}
RN12O2	1.66×10^{35}	3.50×10^{32}	5.80×10^{34}	1.59×10^{33}	6.86×10^{33}
RN15O2	8.60×10^{32}	7.13×10^{30}	7.73×10^{32}	1.87×10^{31}	7.92×10^{31}
RN18O2	8.84×10^{31}	1.62×10^{28}	1.30×10^{32}	2.48×10^{30}	8.52×10^{30}
RN15AO2	2.53×10^{34}	2.28×10^{32}	2.77×10^{34}	5.54×10^{32}	3.12×10^{33}
RN18AO2	5.11×10^{33}	2.95×10^{30}	1.63×10^{33}	6.61×10^{31}	1.56×10^{32}
CH3CO3	4.17×10^{36}	7.97×10^{34}	1.38×10^{36}	1.01×10^{36}	2.85×10^{35}
C2H5CO3	9.58×10^{36}	1.00×10^{33}	1.25×10^{34}	8.03×10^{33}	2.92×10^{33}
HOCH2CO3	4.33×10^{35}	7.98×10^{33}	1.23×10^{35}	1.02×10^{35}	2.46×10^{34}
RN8O2	2.21×10^{35}	1.81×10^{33}	2.18×10^{35}	9.93×10^{33}	3.42×10^{34}
RN11O2	1.40×10^{35}	1.17×10^{33}	1.47×10^{35}	5.31×10^{33}	1.88×10^{34}
RN14O2	7.01×10^{33}	5.47×10^{31}	9.35×10^{33}	3.22×10^{32}	1.00×10^{33}
RN17O2	1.55×10^{33}	1.21×10^{31}	2.04×10^{33}	7.91×10^{31}	1.90×10^{32}
RU14O2	1.79×10^{36}	1.44×10^{33}	1.41×10^{36}	1.07×10^{35}	1.02×10^{35}
RU12O2	3.80×10^{35}	1.67×10^{33}	7.08×10^{35}	1.81×10^{35}	5.34×10^{34}
RU10O2	6.17×10^{35}	4.72×10^{33}	5.19×10^{35}	5.68×10^{34}	4.26×10^{34}
NRN6O2	3.81×10^{31}	3.56×10^{32}	8.12×10^{31}	2.85×10^{31}	2.81×10^{30}
NRN9O2	2.29×10^{32}	1.19×10^{33}	3.73×10^{32}	4.74×10^{31}	9.71×10^{30}

NRN12O2	4.90×10^{34}	2.03×10^{33}	1.54×10^{33}	1.90×10^{32}	3.49×10^{31}
NRU14O2	2.29×10^{34}	2.35×10^{34}	8.63×10^{34}	5.12×10^{34}	1.42×10^{33}
NRU12O2	4.71×10^{34}	6.61×10^{32}	7.80×10^{34}	1.81×10^{33}	5.62×10^{33}
RTN28O2	8.60×10^{34}	1.10×10^{32}	5.33×10^{34}	7.38×10^{32}	3.95×10^{33}
NRTN28O2	3.59×10^{34}	1.24×10^{34}	3.91×10^{34}	3.07×10^{33}	8.43×10^{32}
RTN26O2	1.94×10^{35}	2.58×10^{33}	3.46×10^{34}	4.09×10^{34}	6.69×10^{33}
RTN25O2	2.21×10^{35}	3.83×10^{33}	2.77×10^{35}	1.59×10^{34}	1.99×10^{34}
RTN24O2	1.83×10^{35}	3.77×10^{33}	2.35×10^{35}	8.61×10^{31}	1.82×10^{34}
RTN23O2	1.70×10^{35}	2.62×10^{33}	2.18×10^{35}	4.97×10^{31}	1.83×10^{34}
RTN14O2	1.69×10^{35}	1.96×10^{33}	1.92×10^{35}	4.74×10^{33}	1.84×10^{34}
RTN10O2	1.17×10^{35}	1.19×10^{33}	1.11×10^{35}	5.94×10^{33}	1.28×10^{34}
RTX28O2	9.31×10^{34}	2.58×10^{32}	8.47×10^{34}	6.72×10^{33}	5.83×10^{33}
NRTX28O2	2.78×10^{34}	7.71×10^{33}	3.86×10^{34}	1.71×10^{33}	1.91×10^{33}
RTX24O2	7.44×10^{34}	6.56×10^{32}	7.29×10^{34}	8.30×10^{32}	5.49×10^{33}
RTX22O2	4.84×10^{34}	3.85×10^{32}	7.52×10^{34}	4.17×10^{32}	5.97×10^{33}
RU10AO2	1.93×10^{34}	7.39×10^{30}	1.61×10^{34}	2.44×10^{35}	1.07×10^{33}
MACO3	1.04×10^{35}	5.90×10^{32}	4.76×10^{34}	2.77×10^{34}	4.05×10^{33}
DHPR12O2	5.25×10^{33}	4.39×10^{30}	4.18×10^{33}	2.36×10^{35}	3.07×10^{32}

Table S5. Losses of CH_3O_2, $ISOPO_2$ and $MONOTERPO_2$ by different species

Species	CH_3O_2 (s^{-1})	$ISOPO_2$ (s^{-1})	$MONOTERPO_2$ (s^{-1})
NO	3.14×10^{-3}	2.60×10^{-2}	4.89×10^{-2}
NO_3	7.01×10^{-5}	1.23×10^{-3}	2.10×10^{-3}
HO_2	1.18×10^{-3}	2.25×10^{-2}	4.01×10^{-3}
RO_2	2.11×10^{-4}	2.86×10^{-4}	2.39×10^{-4}
OH	3.68×10^{-4}	2.58×10^{-3}	4.41×10^{-3}

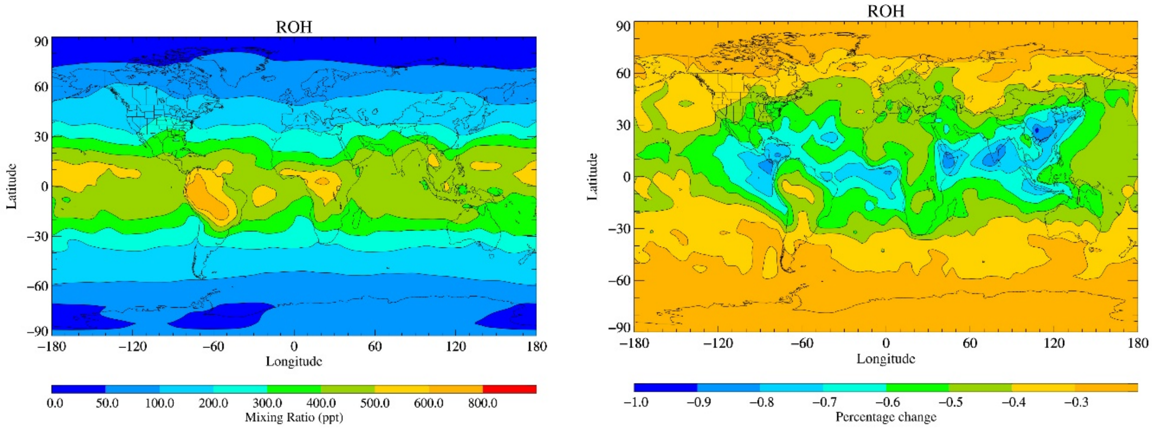

(a) (b)

Figure S1. (a) Annual ROH mixing ratios simulated by STOCH-RO2-OH-B, (b) Annual ROH mixing ratios change from STOCH-RO2-OH-D to STOCH-RO2-OH-B

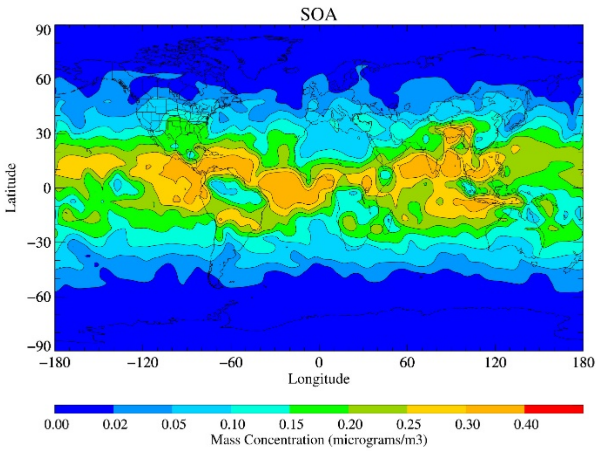

Figure S2. Annual ROOOH mixing ratios simulated by STOCH-RO2-OH-D-OA

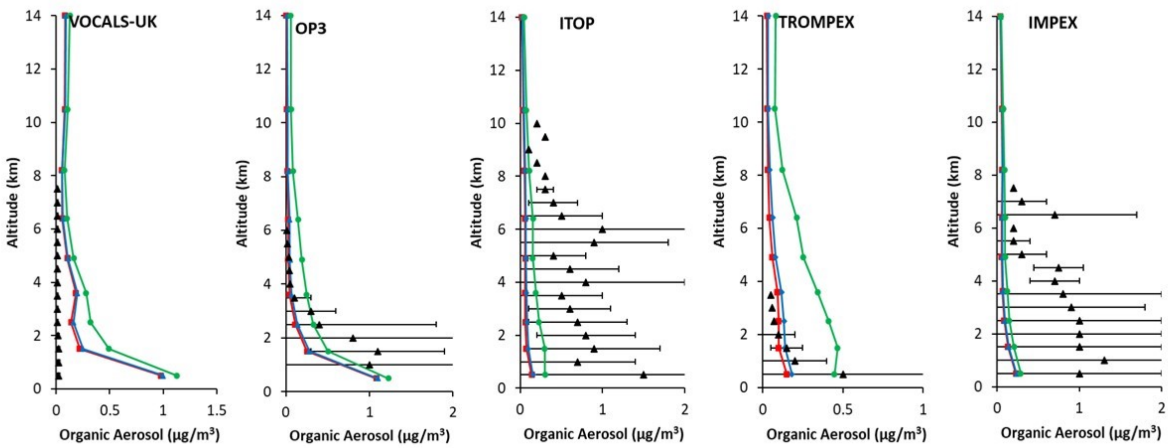

Figure S3. Vertical profiles for measured and modelled organic aerosols for selected remote sites. The red, blue, and green lines represent mean model values of OA produced by STOCH-Base, STOCH-RO2-OH, and STOCH-RO2-OH-D, respectively. The black triangles represent the flight campaign measurement OA data for remote sites compiled from Heald et al.[30] and the black bars represent the measurement variability.

References

1. X. Ren, W. H. Brune, A. Oliger, A. R. Metcalf, J. B. Simpas, T. Shirley, J. J. Schwab, C, Bai, U. Roychowdhury, Y. Li, C. Cai, K. L. Demerjian, Y. He, X. Zhou, H. Gao and J. Hou, OH, HO_2, and OH reactivity during the PMTACS-NY Whiteface Mountain 2002 campaign: Observations and model comparison, *J. Geophys. Res.-Atmos.*, 2006a, **111**, 1–12.

2. T. A. Kovacs, W. H. Brune, H. Harder, M. Martinez, J. B. Simpas, G. J. Frost, E. Williams, T. Jobson, C. Stroud, V. Young, A. Fried and B. Wert, Direct measurements of urban OH reactivity during Nashville SOS in summer 1999, *J. Environ. Monit.*, 2003, **5**, 68–74.

3. P. M. Edwards, M. J. Evans, K. L. Furneaux, J. Hopkins, T. Ingham, C. Jones, J. D. Lee, A. C. Lewis, S. J. Moller, D. Stone, L. K. Whalley and D. E. Heard, OH reactivity in a South East Asian tropical rainforest during the Oxidant and Particle Photochemical Processes (OP3) project, *Atmos. Chem. Phys.*, 2013, **13**, 9497–9514.

4. A. C. Nölscher, A. M. Yañez-Serrano, S. Wolff, A. C. de Araujo, J. V. Lavric, J. Kesselmeier and J. Williams, Unexpected seasonality in quantity and composition of Amazon rainforest air reactivity, *Nature Commun.*, 2016, **7**, 10383.

5. J. D. Lee, J. C. Young, K. A. Read, J. F. Hamilton, J. R. Hopkins, A. C. Lewis, B. J. Bandy, J. Davey, P. Edwards, T. Ingham, D. E. Self, S. C. Smith, M. J. Pilling and D. E. Heard, Measurement and calculation of OH reactivity at a United Kingdom coastal site, *J. Atmos. Chem.*, 2009, **64**, 53–76.

6. K. Lu, Y. Zhang, H. Su, T. Brauers, C. C. Chou, A. Hofzumahaus, S. C. Liu, K. Kita, Y. Kondo, M. Shao, A. Wahner, J. Wang, X. Wang and T. Zhu, Oxidant (O_3 + NO_2) production processes and formation regimes in Beijing, *J. Geophys. Res. Atmos.*, 2010, **115**, D07303.

7. S. Lou, F. Holland, F. Rohrer, K. Lu, B. Bohn, T. Brauers, C. C. Chang, H. Fuchs, R. Häseler, K. Kita, Y. Kondo, X. Li, M. Shao, L. Zeng, A. Wahner, Y. Zhang, W. Wang and A. Hofzumahaus, Atmospheric OH reactivities in the Pearl River Delta – China in summer 2006: measurement and model results, *Atmos. Chem. Phys.*, 2010, **10**, 11243–11260.

8. V. Sinha, J. Williams, J. N. Crowley and J. Lelieveld, The comparative reactivity method-a new tool to measure total OH reactivity in ambient air, *Atmos. Chem. Phys.*, 2008, **8**, 2213–2227.

9. Y. F. Elshorbany, J. Kleffmann, A. Hofzumahaus, R. Kurtenbach, P. Wiesen, T. Brauers, B. Bohn, H. P. Dorn, H. Fuchs, F. Holland, F. Rohrer, R. Tillmann, R. Wegener, A. Wahner, Y. Kanaya, A. Yoshino, S. Nishida, Y. Kajii, M. Martinez, D. Kubistin, H. Harder, J. Lelieveld, T. Elste, C. Plass-Dlmer, G. Stange, H. Berresheim and U. Schurath, HO_x budgets during HOxComp: A case study of HO_x chemistry under NO_x-limited conditions, *J. Geophys. Res.-Atmos.*, 2012, **117**, 1–16.

10. Y. Yang, M. Shao, S. Keßel, Y. Li, K. Lu, S. Lu, J. Williams, Y. Zhang, L. Zeng, A. C. Nölscher, Y. Wu, X. Wang and J. Zheng, How the OH reactivity affects the ozone production efficiency: case studies in Beijing and Heshan, China, *Atmos. Chem. Phys.*, 2017, **17**, 7127–7142.

11. N. Zannoni, V. Gros, R. Sarda Esteve, C. Kalogridis, V. Michoud, S. Dusanter, S. Sauvage, N. Locoge, A. Colomb and B. Bonsang, Summertime OH reactivity from a receptor coastal site in the Mediterranean Basin, *Atmos. Chem. Phys.*, 2017, **17**, 12645– 12658.

12. X. Ren, H. Harder, M. Martinez, R. L. Lesher, A. Oliger, T. Shirley, J. Adams, J. B. Simpas and W. H. Brune, HO_x concentrations and OH reactivity observations in New York City during PMTACS-NY2001, *Atmos. Environ.*, 2003, **37**, 3627–3637.

13. X. Ren, W. H. Brune, J. Mao, M. J. Mitchell, R. L. Lesher, J. B. Simpas, A. R. Metcalf, J. J. Schwab, C. Cai, Y. Li, K. L. Demerjian, H. D. Felton, G. Boynton, A. Adams, J. Perry, Y. He, X. Zhou and J. Hou, Behavior of OH and HO_2 in the winter atmosphere in New York City, *Atmos. Environ.*, 2006b, **40**, 252–263.

14. X. Ren, W. H. Brune, C. A. Cantrell, G. D. Edwards, T. Shirley, A. R. Metcalf and R. L. Lesher, Hydroxyl and peroxy radical chemistry in a rural area of central Pennsylvania: Observations and model comparisons, *J. Atmos. Chem.*, 2005, **52**, 231–257.

15. T. R. Shirley, W. H. Brune, X. Ren, J. Mao, R. Lesher, B. Cardenas, R. Volkamer, L. T. Molina, M. J. Molina, B. Lamb, E. Velasco, T. Jobson and M. Alexander, Atmospheric oxidation in the Mexico City Metropolitan Area (MCMA) during April 2003, *Atmos. Chem. Phys.*, 2006, **6**, 2753– 2765.

16. J. Mao, X. Ren, S. Chen, W. H. Brune, Z. Chen, M. Martinez, H. Harder, B. Lefer, B. Rappenglück, J. Flynn and M. Leuchner, Atmospheric oxidation capacity in the summer of Houston 2006: Comparison with summer measurements in other metropolitan studies, *Atmos. Environ.*, 2010, **44**, 4107–4115.

17. C. Dolgorouky, V. Gros, R. Sarda-Esteve, V. Sinha, J. Williams, N. Marchand, S. Sauvage, L. Poulain, J. Sciare and B. Bonsang, Total OH reactivity measurements in Paris during the 2010 MEGAPOLI winter campaign, *Atmos. Chem. Phys.*, 2012, **12**, 9593– 9612.

18. R. F. Hansen, M. Blocquet, C. Schoemaecker, T. Léonardis, N. Locoge, C. Fittschen, B. Hanoune, P. S. Stevens, V. Sinha and S. Dusanter, Intercomparison of the comparative

reactivity method (CRM) and pump-probe technique for measuring total OH reactivity in an urban environment, *Atmos. Meas. Tech.*, 2015, **8**, 4243–4264.

19. L. K. Whalley, D. Stone, B. Bandy, R. Dunmore, J. F. Hamilton, J. Hopkins, J. D. Lee, A. C. Lewis and D. E. Heard, Atmospheric OH reactivity in central London: observations, model predictions and estimates of in situ ozone production, *Atmos. Chem. Phys.*, 2016, **16**, 2109–2122.

20. R. F. Hansen, S. M. Griffith, S. Dusanter, P. S. Rickly, P. S. Stevens, S. B. Bertman, M. A. Carroll, M. H. Erickson, J. H. Flynn, N. Grossberg, B. T. Jobson, B. L. Lefer and H. W. Wallace, Measurements of total hydroxyl radical reactivity during CABINEX 2009 – Part 1: field measurements, *Atmos. Chem. Phys.*, 2014, **14**, 2923–2937.

21. V. Sinha, J. Williams, J. Lelieveld, T. M. Ruuskanen, M. K. Kajos, J. Patokoski, H. Hellen, H. Hakola, D. Mogensen, M. Boy, J. Rinne and M. Kulmala, OH reactivity measurements within a boreal forest: Evidence for unknown reactive emissions, *Environ. Sci. Technol.*, 2010, **44**, 6614–6620.

22. A. C. Nölscher, J. Williams, V. Sinha, T. Custer, W. Song, A. M. Johnson, R. Axinte, H. Bozem, H. Fischer, N. Pouvesle, G. Phillips, J. N. Crowley, P. Rantala, J. Rinne, M. Kulmala, D. Gonzales, J. Valverde-Canossa, A. Vogel, T. Hoffmann, H. G. Ouwersloot, J. Vilà-Guerau de Arellano, J. Lelieveld, Summertime total OH reactivity measurements from boreal forest during HUMPPA-COPEC 2010, *Atmos. Chem. Phys.*, 2012, **12**, 8257–8270.

23. Y. Nakashima, S. Kato, J. Greenberg, P. Harley, T. Karl, A. Turnipseed, E. Apel, A. Guenther, J. Smith and Y. Kajii, Total OH reactivity measurements in ambient air in a southern Rocky mountain ponderosa pine forest during BEACHON-SRM08 summer campaign, *Atmos. Environ.*, 2014, **85**, 1– 8.

24. N. Zannoni, V. Gros, M. Lanza, R. Sarda, B. Bonsang, C. Kalogridis, S. Preunkert, M. Legrand, C. Jambert, C. Boissard and J. Lathiere, OH reactivity and concentrations of biogenic volatile organic compounds in a Mediterranean forest of downy oak trees, *Atmos. Chem. Phys.*, 2016, **16**, 1619–1636.

25. J. Kaiser, K. M. Skog, K. Baumann, S. B. Bertman, S. B. Brown, W. H. Brune, J. D. Crounse, J. A. de Gouw, E. S. Edgerton, P. A. Feiner, A. H. Goldstein, A. Koss, P. K. Misztal, T. B. Nguyen, K. F. Olson, J. M. St. Clair, A. P. Teng, S. Toma, P. O. Wennberg, R. J. Wild, L. Zhang and F. N. Keutsch, Speciation of OH reactivity above the canopy of an isoprene-dominated forest, *Atmos. Chem. Phys.*, 2016, **16**, 9349– 9359.

26. J. Mao, X. Ren, L. Zhang, D. M. Van Duin, R. C. Cohen, J. -H. Park, A. H. Goldstein, F. Paulot, M. R. Beaver, J. D. Crounse, P. O. Wennberg, J. P. DiGangi, S. B. Henry, F. N. Keutsch, C. Park, G. W. Schade, G. M. Wolfe, J. A. Thornton and W. H. Brune, Insights into hydroxyl measurements and atmospheric oxidation in a California forest, *Atmos. Chem. Phys.*, 2012, **12**, 8009–8020.

27. J. Mao, X. Ren, W. H. Brune, J. R. Olson, J. H. Crawford, A. Fried, L. G. Huey, R. C. Cohen, B. Heikes, H. B. Singh, D. R. Blake, G. W. Sachse, G. S. Diskin, S. R. Hall and R. E.

Shetter, Airborne measurement of OH reactivity during INTEX-B, *Atmos. Chem. Phys.*, 2009, **9**, 163–173.

28. E. Y. Pfannerstill, N. Wang, A. Edtbauer, E. Bourtsoukidis, J. N. Crowley, D. Dienhart, P. G. Eger, L. Ernle, H. Fischer, B. Hottmann, J. -D. Paris, C. Stönner, I. Tadic, D. Walter, J. Lelieveld and J. Williams, Shipborne measurements of total OH reactivity around the Arabian Peninsula and its role in ozone chemistry, *Atmos. Chem. Phys.*, 2019, **19**, 11501–11523.

29. G. Yang, J. Huo, L. Wang, Y. Wang, S. Wu, L. Yao and Q. Fu, Total OH reactivity measurements in a suburban site of Shanghai, *J. Geophys. Res. Atmos.*, 2022, **127**, e2021JD035981.

30. C. L. Heald, H. Coe, J. L. Jimenez, R. J. Weber, R. Bahreini, A. M. Middlebrook, L. M. Russell, M. Jolleys, T. -M. Fu, J. D. Allan, K. N. Bower, G. Capes, J. Crosier, W. T. Morgan, N. H. Robinson, P. I. Williams, M. J. Cubison, P. F. DeCarlo and E. J. Dunlea, Exploring the vertical profile of atmospheric organic aerosol: Comparing 17 aircraft field campaigns with a global model, *Atmos. Chem. Phys.*, 2011, **11**, 12673–12696.